ISOTOPE RATIO TRIANGULATION: A METHOD FOR DETERMINING URANIUM ISOTOPE RATIOS AND APPLICATION TO THE SEARCH FOR URANIUM ISOTOPE ANOMALIES IN THE MINERAL TITANITE

A Thesis

by

JOSEPH ROGER HILL

Submitted to the Office of Graduate and Professional Studies of
Texas A&M University
in partial fulfillment of the requirements for the degree of

MASTER OF SCIENCE

Chair of Committee,	Brent V. Miller
Committee Members,	Franco Marcantonio
	Charles M. Folden III
Head of Department,	John R. Giardino

December 2014

Major Subject: Geology

ABSTRACT

The U-Pb dating methods used in many geochronology laboratories take advantage of a mixed ^{235}U-^{233}U spike for precise uranium isotopic measurements and current data reduction algorithms assume a uniform $^{238}U/^{235}U$ value of 137.88. Recent re-evaluation of the isotope ratio of "natural" uranium value used in geochronology has called into question both this value and its constancy in U-bearing minerals, most notably titanite, formed in high-temperature magmatic and metamorphic settings. A ^{233}U-^{236}U spike may be used for direct determination of the uranium isotopic composition, but this spike is not widely used and in some labs where it is, the $^{238}U/^{235}U$ ratio is not independently measured. Isotope Ratio Triangulation (IRT) is a new and effective method for determining $^{238}U/^{235}U$ values analyzed with the more common ^{235}U-^{233}U uranium spike. This method leverages the effect of mass-spectrometer-induced isotopic fractionation in three measured ratios to determine $^{238}U/^{235}U$ values. Graphically, this is represented by three intersecting lines for fractionation factors calculated at varying $^{238}U/^{235}U$ ratios, hence the term "triangulation".

The IRT method is here applied to 43 aliquots of 23 titanite samples from a wide range of geologic settings, ages and locations. Of these, five aliquots yielded anomalously high $^{238}U/^{235}U$ ratios. Three were likely to be entirely uranium blank. Two other samples yielded anomalously high $^{238}U/^{235}U$ values. Both were roughly 2.5 Ga and coincide with the Archean to early Proterozoic oxidation of the world's oceans termed

the “Great Oxidation Event”. Low temperature redox reactions have been shown to have a similar depletion effect.

These results demonstrate the accuracy of this new method, which can be used to efficiently scan large volumes of existing geochronologic data in search of anomalous U isotope ratios. In addition, results indicate that laboratory blank in the TAMU radiogenic isotope laboratory is not of “natural” composition. Finally, these results are more consistent with a “natural” uranium composition of $^{238}U/^{235}U = 137.88$ than the recently suggested value of 137.818.

DEDICATION

Travis, Justin, Nazario, Doc B and Brad

See you on the other side

ACKNOWLEDGEMENTS

First and foremost, I would like to thank my advisor and committee chair, Dr. Brent Miller. This project has been personally and professionally enriching and I am grateful to have had the opportunity to work for and with him. I would also like to acknowledge the faculty and staff of the Texas A&M Geology Department for their patience and support, many of whom have been like family to me.

TABLE OF CONTENTS

Page

LIST OF FIGURES

Page

INTRODUCTION

The method currently used to determine the most precise $^{238}U/^{235}U$ ratios and elemental concentrations for geochronology involves the application of a ^{236}U-^{233}U uranium spike which allows for the direct calculation of that ratio (Brennecka et al. 2010, Hiess et al. 2012). However, a ^{235}U-^{233}U spike has been widely used in many geochronology laboratories to determine high precision U concentrations. Regardless of spike, current data reduction methods rely on the assumption of the $^{238}U/^{235}U$ ratio being a constant 137.88 (Jaffey et al. 1971), a value which is used without error. This paper outlines a method for determining precise $^{238}U/^{235}U$ ratios using a ^{235}U-^{233}U uranium spike. This new method is then applied to a selection of titanite samples to demonstrate its effectiveness and to explore the possibility of uranium isotope anomalies in this mineral.

The decay of ^{238}U(parent) into ^{206}Pb(daughter) and ^{235}U(parent) into ^{207}Pb(daughter) occurs according to the equation:

$$D = D_0 + N(e^{\lambda t} - 1) \qquad \text{Eq.1}$$

where

D = the number of atoms of daughter isotope currently in the sample

D_0 = the number of atoms of daughter isotope originally in the sample

N = the number of atoms of the parent isotope currently in the sample

λ = the decay constant (^{235}U=9.8485X10^{-10}/yr; ^{238}U=1.55125X10^{-10}/ yr)

(Steiger and Jager 1977)

t = the age of the system

This equation can be solved for t if the present-day ratios of either $^{235}U/^{207}Pb$ or $^{238}U/^{206}Pb$ can be measured in geological samples by isotope-ratio mass spectrometry. Thermal ionization mass spectrometers (TIMS), however, measure only isotope ratios of the same element. Current practice, therefore, is to introduce tracer isotopes into the sample in order to determine atomic abundances and thus isotope ratios of U and Pb. The calculations for determining U/Pb isotope ratios assume that the present-day $^{238}U/^{235}U$ isotope ratio is constant in all samples, and thus does not require the ratio be measured directly. Since Jaffey et al. (1971), a value of 137.88 has been used in geochronology. This ratio is treated as a universal constant in widely used data reduction algorithms (McLean, Bowring, and Bowring 2011, Schmitz and Schoene 2007). The most widely used tracer solutions in geochronology employ the "isotope dilution" method in which ^{233}U and an excess of ^{235}U is added to a sample in order to both correct for mass bias within the mass spectrometer and to allow calculation of the ^{238}U isotopic abundance (Mattinson 2005b, a).

Recent work re-evaluating the natural $^{238}U/^{235}U$ ratio for geochronologic purposes has focused on U contained in the important geochronometer mineral zircon (Hiess et al. 2012) and has concluded that the natural "bulk Earth" $^{238}U/^{235}U$ value is better estimated

as 137.818 ± 0.045 (2σ). Data from the same study show a generally small natural variability in this ratio with the exception of two titanite samples, which show a wide variation from 137.818 (by up to 4890 ppm). Other geochronology minerals have yet to be evaluated fully; as Hiess et al. (2012), noted "Other phases, such as monazite and titanite, require further assessment of their $^{238}U/^{235}U$ variability."

The purpose of this research project is to develop and test a new method for determining the $^{238}U/^{235}U$ isotope ratio using a ^{235}U-^{233}U spike in the mineral titanite from a variety (Fig. 1) of igneous rocks from different locations (Fig. 2), geologic settings and of different ages.

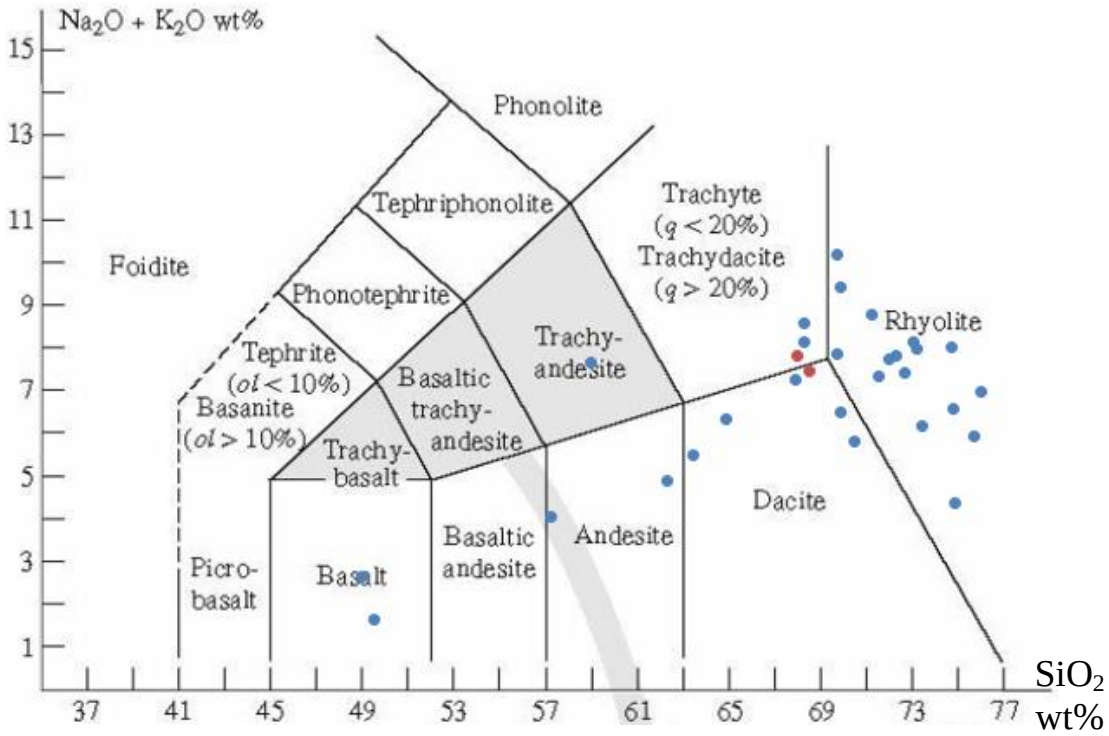

Figure 1 Total-alkali vs silica diagram (Le Bas et al. 1986) illustrating rock compositions for igneous and metaigneous samples used in this study (blue dots). The Fish Canyon Tuff (red dots) is dacitic by bulk composition.

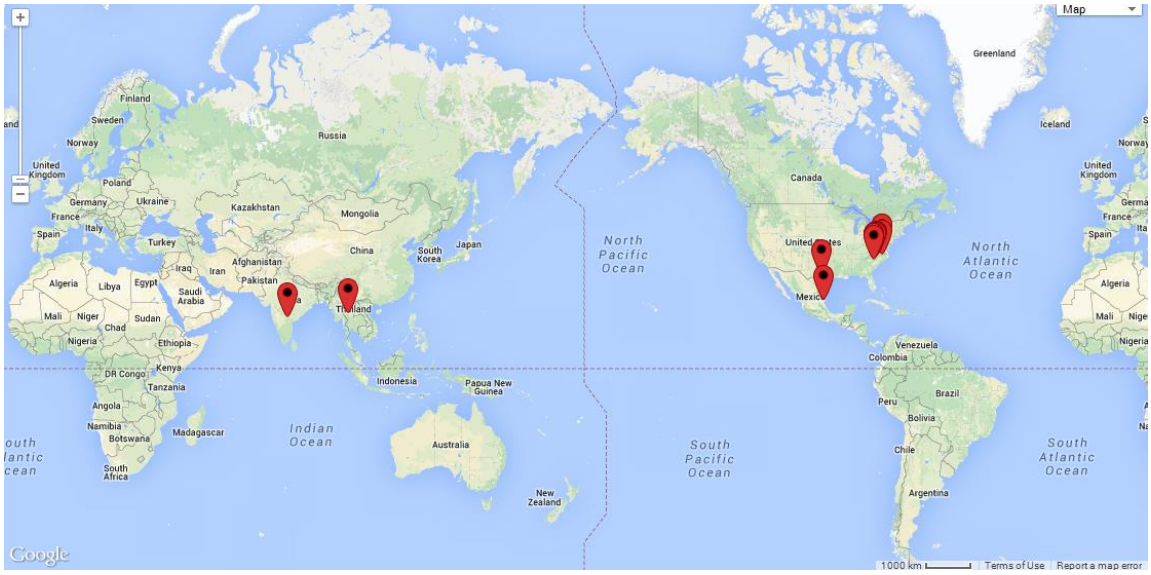

Figure 2 Global distribution of titanite samples used in this study. Samples come mainly from central Texas, Virginia, and North and South Carolina; but a few samples also come from Mexico, India and Thailand.

Background

Uranium exists in three common naturally occurring isotopes: ^{234}U, ^{235}U, and ^{238}U; the latter two are primordial and ^{234}U is a moderately long-lived daughter of ^{238}U. With some minor exceptions described below, it was believed these isotopes occur in fixed ratios to each other (Cowan and Adler 1976). Because of uranium's large mass and the small mass difference between ^{238}U and ^{235}U, mass-dependent fractionation in high-temperature geologic systems (e.g., magmatic and regional metamorphic settings) was previously thought to be negligible (Stirling, Andersen, Potter, et al. 2007). Recent high-precision U isotope measurements, however, show variations in comagmatic minerals,

suggesting that U isotope fractionation is either taking place within or inherited into magmatic systems (Hiess et al. 2012).

Anomalous U isotope ratios found in other geological settings are mostly related to low-temperature redox reactions. These anomalies result from fractionation due to changes in nuclear volume and electron density distributions (Schauble 2007). This nuclear field shift is caused by a change in oxidation state, this type of fractionation is density dependent and mass independent (Stirling, Andersen, Potter, et al. 2007, Stirling, Andersen, Warthmann, et al. 2007). Brennecka et al. (2010) showed that uranium deposited in low temperature environments is, on average, 0.4‰ isotopically heavier than its high temperature and non-redox counterparts. Brennecka et al. (2008) also demonstrated that uranium isotopes fractionate during adsorption to Mn-oxyhydroxides resulting in fractionation between ferromanganese crusts and seawater. This type of fractionation is mostly likely the result of difference in coordination environment between dissolved and adsorbed U (Brennecka et al. 2008). Fractionation of this kind creates ferromanganese sediment which is enriched in ^{235}U. Permil-level variability has also been documented in the other heavy elements such as thallium (Nielsen et al. 2006, Nielsen et al. 2005) and mercury (Smith et al. 2005).

The accepted $^{238}U/^{235}U$ value of 137.88, which has been used in geochronology for the last 35 years, has recently been called into question. Hiess et al. (2012) propose a new value of 137.818 ± 0.045 (2σ). Hiess et al. (2012) tested 45 zircon samples, 44 of which

fell into a normal distribution around 137.818. A Miocene Table Cape zircon from Tasmania, yielded a ratio of 138.283 ± 0.022 (2σ), thought to be derived from a unique, isotopically heavy reservoir derived from the mantle and sourced from a local alkaline volcanic field. Titanite from the Fish Canyon tuff and a metamorphic megacryst (their sample BLR-1), yielded ratios of 138.490 ± 0.022 (2σ) and 138.068 ± 0.022 (2σ), respectively (Hiess et al. 2012). The Oligocene Fish Canyon Tuff was produced during one of the largest known volcanic eruptions in Earth's history and is remarkably homogenous for its size, roughly 5000 km^3 and although it is dacitic in bulk composition due to its phenocryst content (Lipman, Dungan, and Bachmann 1997), its matrix is rhyolitic (SiO_2 75%). The Fish Canyon Tuff is a crystal-rich quartz latite with roughly 40% phenocrysts formed from a granitic magma; Fe-Ti geothermometers indicate a tuff outflow temperature of roughly 800°C (Whitney and Stormer 1985). It is notable that zircons from the Fish Canyon tuff do not show anomalous U isotopic composition.

Recent advances in sample preparation, isotope ratio mass spectrometry, and gravimetric calibration of tracers for isotope dissolution methods have made it possible to measure the precision of an individual U-Pb or Pb-Pb age determination to better than 0.1% (Mattinson 2010, Schoene et al. 2006). Uranium isotope fractionation, if it is common in geological materials used in geochronology, has serious implications as the assumption of a constant $^{238}U/^{235}U$ ratio is built into most data reduction schemes. For TIMS analyses, it is necessary to spike a sample with a known concentration of an isotopically enriched tracer solution, i.e., ^{233}U or ^{236}U, in order to determine U concentration in a

geologic sample. Variations in this ratio will require the adjustment of results in previous instrumental and trace calibration efforts (Condon et al. 2010) and will result in small systematic errors in geochronology results which will need to be adjusted in order to be more accurate. It is therefore important to determine if the variation in titanite is common, and if so to what extent isotope ratio variations exist. If natural variation is common in titanite, it will be necessary to determine the cause, as there is not currently a good geochemical explanation for such variation.

Titanite is an important geochronometer because it is a common accessory mineral in a wide range of igneous and metamorphic rocks and is widely used in the amphibolite-facies as a geochronometer. Like zircon, the titanite crystal structure will selectively incorporate trace amounts of U (Tilton 1968). Scott and Onge (1995) suggest that 660-700°C represents a minimum closing temperature and that titanite U-Pb ages can be used for this T range on P-T-t paths. Titanite ages provide vital information for determining the style and timing of exhumation and cooling in metamorphic terrains and to constrain continent-subduction models (Kylander-Clark, Hacker, and Mattinson 2008). Because of its high closing temperature, U-Pb dating of titanite is also useful in determining the timing of amphibolite-facies metamorphic overprints and related tectonic events (Tucker et al. 2004).

METHODS

Mineral Separation

Whole rock samples are crushed, disaggregated and pulverized before having their mineral constituents separated in a multistage process which includes a Wilfely table, heavy liquids and high field magnets. The final stage of mineral separation is individual selection using a binocular microscope. Titanite samples are chosen based on size, shape (how intact the crystal is), and clarity (if the sample free of inclusions and fractures). All samples are photographed before moving onto the next stage of sample preparation. All samples are thoroughly cleaned upon arrival as is all lab equipment before and after each use to minimize the possibility of external or cross contamination.

Sample Preparation and Chemistry

Samples are dissolved before having their uranium and lead components separated and purified in a multistep process based on (Mattinson 2005b) with appropriate modifications for titanite samples compared to zircon, which was studied in the reference. High-purity HF, HCl, HBr and H_3PO_4 acids were purified according to the methods described in (Mattinson 1972). Dissolution and separation chemistry are conducted in a Class 100 (<100 particles >0.3 μm per ft^3 air) ultra-clean laboratory. All Teflon capsules were pre-cleaned with high molarity HNO_3, HCl and HF acids, respectively, and allowed to sit on a hotplate at 90°C in a process that takes no less than a week. This cleaning process removes any of the previous sample and leaches out any U or Pb which may have been introduced in the Teflon during is manufacture. Pipette

tips are also replaced after each sample and at each step to prevent cross contamination. An internally calibrated, mixed ^{205}Pb-^{233}U-^{235}U spike is added to dissolved samples for U-Pb analysis. U and Pb are separated from contaminants using chromatographic techniques as described in (Mattinson 2005b). Samples are then dried down then loaded onto a high-purity rhenium filament. Freshly distilled reagents and careful sample preparation have reduced procedural blanks to <2 pg Pb per sample, and U blank contents were consistently undetectable (<0.1 pg) and thus are only sporadically analyzed.

TIMS Analysis

All isotope-ratio measurements are conducted on a ThermoFisher Triton thermal-ionization mass spectrometer housed in the R. Ken Williams Radiogenic Isotope Geosciences Laboratory at Texas A&M University. Uranium isotope masses ^{233}U, ^{235}U and ^{238}U are measured simultaneously in three Faraday detectors in static collection mode with amplifier rotation. Lead isotope masses ^{204}Pb, ^{205}Pb, ^{206}Pb, ^{207}Pb and ^{208}Pb are measured by either peak-hopping on the secondary electron multiplier (SEM) or with two-step Faraday/SEM analysis that allows for within-run gain calibration between the SEM and central Faraday detector.

Data Processing and Reduction

Raw data are first analyzed using Tripoli 4.7 to carefully check for data consistency and quality. Data is reduced within this program to useful portions that do not include the

wildly varying ratios seen during sample warm up and at exhaustion. The "YourLab" algorithms of (Schmitz and Schoene 2007, Schoene et al. 2006) are used for data reduction and IsoPlot 3.00 is used for plotting diagrams.

Precision of Measurement

Figure 3 shows "proof of concept" data to demonstrate that the facilities in the TAMU Radiogenic Isotope Geochemistry Laboratory are capable of making measurements with the internal precision and external reproducibility necessary to resolve the $^{238}U/^{235}U$ variations seen in the Fish Canyon Tuff and BLR-1. Spiked samples were measured with an average internal precision of 41 ppm and an external reproducibility of 138 ppm while unspiked samples demonstrated 52 ppm internal and 800 ppm external. Internal precision refers to an individual measurement and external precision refers to a set of measurements, all with a 2σ confidence level. The average internal precision achieved falls well within the 4890 ppm difference measured in the Fish Canyon titanite.

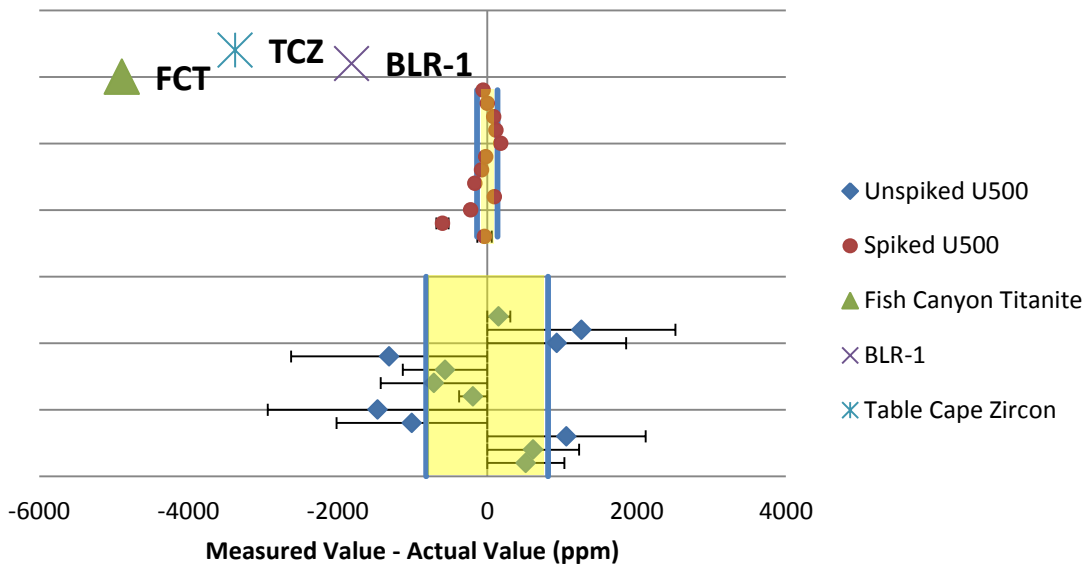

Figure 3 Resolvability of $^{238}U/^{235}U$ variations demonstrated using the isotopic standard U500 for spiked (red dots) and unspiked (blue diamonds) analyses. Unspiked analyses are corrected for fractionation using a laboratory-average fractionation factor of 0.08%/AMU. Spiked analyses are corrected for fractionation using the measured $^{233}U/^{235}U$ ratio. Error bars represent the precision of individual measurements while the shaded areas represent average external reproducibility.

Fractionation Correction and $^{238}U/^{235}U$ Anomaly

Three isotope ratios are measured when samples are spiked with a mixed $^{233}U/^{235}U$ tracer solution: $^{238}U/^{233}U$, $^{233}U/^{235}U$, and $^{238}U/^{235}U$. The ^{233}U isotope is manmade; all of the ^{233}U in the sample is derived from the spike. Conversely, the ^{238}U measured is overwhelmingly from the sample with a small contribution from the spike and the opposite is true for ^{235}U (Fig. 4). A complication of measuring these ratios by TIMS is that lighter isotopes require less energy to ionize, resulting in mass dependent fractionation. Precise determination of any measured ratio requires accurate correction

for mass dependent fractionation (FU, Fig. 4). A linear fractionation law is used to make this correction and though the fractionation is not strictly linear McLean, Bowring, and Bowring (2011) noted that linear law is virtually indistinguishable from exponential or power law when the magnitude of the isotopic fractionation is low, roughly 0.1% (see Discussion section for additional detail).

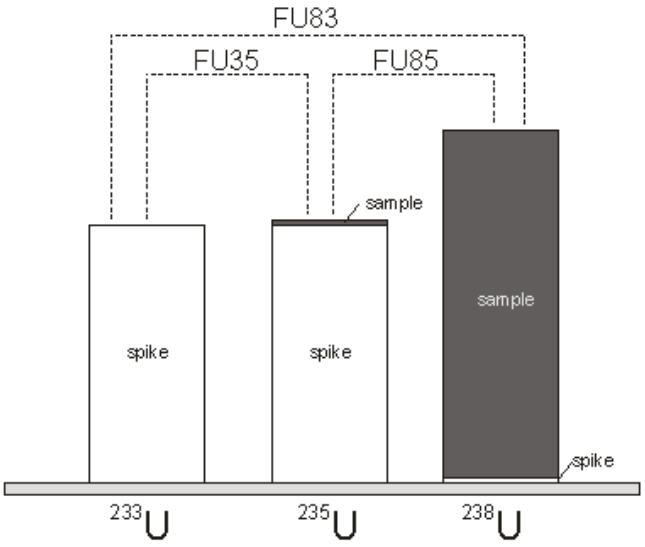

Figure 4 Schematic depiction of relative proportions of sample and spike U isotopes for analyses conducted with a mixed $^{233}U/^{235}U$ spike and fractionation during the measurement of the ratios (contribution from laboratory blank is not depicted here).

According to the linear fractionation law (McLean, Bowring, and Bowring 2011, Young, Galy, and Nagahara 2002) the following three equations can be written to correct the three measured isotope ratios for fractionation:

$$\left(\frac{^{238}\mathrm{U}}{^{235}\mathrm{U}}\right)_t = \left(\frac{^{238}\mathrm{U}}{^{235}\mathrm{U}}\right)_m \times (1 + 3FU_{85})$$

Eq.2a

$$\left(\frac{^{233}\mathrm{U}}{^{235}\mathrm{U}}\right)_t = \left(\frac{^{233}\mathrm{U}}{^{235}\mathrm{U}}\right)_m \times (1 - 2FU_{35})$$

Eq.2b

$$\left(\frac{^{238}\mathrm{U}}{^{233}\mathrm{U}}\right)_t = \left(\frac{^{238}\mathrm{U}}{^{233}\mathrm{U}}\right)_m \times (1 + 5FU_{83})$$

Eq. 2c

Where:

FU_{85}, FU_{35}, and FU_{83} are the proportional fractionation factors per atomic mass unit for the measured ratios $^{238}\mathrm{U}/^{235}\mathrm{U}$, $^{233}\mathrm{U}/^{235}\mathrm{U}$, and $^{238}\mathrm{U}/^{233}\mathrm{U}$, respectively, the subscripts *t* and *m* refer to the "true" and "measured ratios", respectively, and in the ideal situation, $FU_{85} = FU_{35} = FU_{83}$

By rearranging to solve for the uranium fractionation factors (*FU*):

$$FU_{85} = \frac{\left[\frac{\left(\frac{^{238}\mathrm{U}}{^{235}\mathrm{U}}\right)_t}{\left(\frac{^{238}\mathrm{U}}{^{235}\mathrm{U}}\right)_m}\right] - 1}{3}$$

Eq. 3a

$$FU_{35} = \frac{\left[\frac{\left(\frac{233U}{235U}\right)_t}{\left(\frac{233U}{235U}\right)_m}\right] - 1}{-2}$$

Eq. 3b

$$FU_{83} = \frac{\left[\frac{\left(\frac{238U}{233U}\right)_t}{\left(\frac{238U}{233U}\right)_m}\right] - 1}{5}$$

Eq. 3c

For ease of calculation, anomalous $^{238}U/^{235}U$ ratios are attributed to an excess or deficit in the molar proportion of ^{238}U, leading to the following relations:

$$\mathbf{238U}_{anom} = \mathbf{238U}_{norm} + \mathbf{238U}_{exdef}$$

Eq. 4a

$$\mathbf{235U}_{norm} = \frac{\mathbf{238U}_{norm}}{137.88}$$

Eq. 4b

Where:

238U is the molar abundance of ^{238}U in the sample

235U is the molar abundance of ^{235}U in the sample

and the subscripts *anom*, *norm* and *exdef* refer to the molar abundance of the isotope in a uranium sample of anomalous isotopic ratio, in a sample of normal or "natural" isotope ratio ($^{238}U/^{235}U$ = 137.88) and the excess or deficit molar abundance of the isotope, respectively.

These relations state that any difference between $^{238}U/^{235}U = 137.88$ and the measured value is due to some amount of molar excess or deficit ^{238}U. It makes no difference whether the excess or deficit is in the molar abundance of ^{238}U or ^{235}U; however assigning it to ^{238}U simplifies the following calculations. A $^{238}U/^{235}U$ greater than 137.88 would have a positive value of $^{\mathbf{238}}\mathbf{U}_{exdef}$, whereas a ratio less than 137.88 would produce a negative value for that variable. In normal isotopic composition uranium $^{\mathbf{238}}\mathbf{U}_{exdef} = 0$ and $^{238}U/^{235}U$ in the sample is 137.88.

Thus, the fractionation equations (Eqs. 2a-2c) can be re-written to include the effect of ^{238}U excess or deficit (anomalous $^{238}U/^{235}U$) as:

$$FU_{85} = \frac{\left[\frac{\left(\frac{\mathbf{238U}_{spk} + \mathbf{238U}_{norm} + \mathbf{238U}_{exdef}}{\mathbf{235U}_{norm} + \mathbf{235}\boldsymbol{U}_{spk}}\right)}{\left(\frac{238U}{235U}\right)_m}\right] - 1}{3}$$

Or, Eq. 5a.1

$$FU_{85} = \frac{\left[\frac{\left(\frac{\mathbf{238U}_{spk} + \mathbf{238U}_{norm} + \mathbf{238U}_{exdef}}{\mathbf{238U}_{norm}/137.88 + \mathbf{235}\boldsymbol{U}_{spk}}\right)}{\left(\frac{238U}{235U}\right)_m}\right] - 1}{3}$$

Eq. 5a.2

$$FU_{35} = \frac{\left[\frac{\left(\frac{\mathbf{233U}_{spk}}{\mathbf{235U}_{norm} + \mathbf{235}\boldsymbol{U}_{spk}}\right)}{\left(\frac{233U}{235U}\right)_m}\right] - 1}{-2}$$

Or, Eq. 5b.1

$$FU_{35} = \frac{\left[\frac{\left(\frac{\mathbf{233U}_{spk}}{\mathbf{238U}_{norm}/137.88 + \mathbf{235}\boldsymbol{U}_{spk}}\right)}{\left(\frac{233U}{235U}\right)_m}\right] - 1}{-2}$$

Eq. 5b.2

$$FU_{83} = \frac{\left[\frac{\left(\frac{\mathbf{238U}_{spk} + \mathbf{238U}_{norm} + \mathbf{238U}_{exdef}}{\mathbf{233}\boldsymbol{U}_{spk}}\right)_t}{\left(\frac{238U}{233U}\right)_m}\right] - 1}{5}$$

Eq. 5c

In equation 5b.2 above, the only unknown is FU35. As shown in Figure 5, FU35 has a negligible sensitivity to relatively large changes in $^{238}U/^{235}U$. Because of this insensitivity, an excellent estimate of $\mathbf{^{238}U}_{norm}$ is possible based on the conventional fractionation correction and spike stripping (McLean, Bowring, and Bowring 2011, Schmitz and Schoene 2007) which have the built-in assumption $^{238}U/^{235}U = 137.88$:

$$FU = \frac{\left[\left(\frac{233\mathrm{U}}{235\mathrm{U}}\right)_{spk} \times \left[\left(\frac{238\mathrm{U}}{235\mathrm{U}}\right)_{m} - \left(\frac{238\mathrm{U}}{235\mathrm{U}}\right)_{norm}\right] + \left(\frac{233\mathrm{U}}{235\mathrm{U}}\right)_{m} \times \left[\left(\frac{238U}{235U}\right)_{norm} - \left(\frac{238U}{235U}\right)_{spk}\right]\right]}{\left[-2 \times \left(\frac{233\mathrm{U}}{235\mathrm{U}}\right)_{m} \times \left[\left(\frac{238\mathrm{U}}{235\mathrm{U}}\right)_{spk} - \left(\frac{238\mathrm{U}}{235\mathrm{U}}\right)_{norm}\right] - 3 \times \left(\frac{233\mathrm{U}}{235\mathrm{U}}\right)_{spk} \times \left(\frac{238\mathrm{U}}{235\mathrm{U}}\right)_{m}\right]}$$

Eq. 6

The calculation of FU83 and FU85 are sensitive to small changes in the molar excess or deficit ^{238}U (Fig. 5). Therefore, the intersection of a line representing FU35 calculated at varying $\mathbf{^{238}U}_{\mathrm{norm}}$ and FU83 calculated at varying $\mathbf{^{238}U}_{\mathrm{exdef}}$ (Fig. 5) indicates the value of $\mathbf{^{238}U}_{\mathrm{exdef}}$ that results in equality of the two FUs, or algebraically:

$$\frac{\left[\frac{\left(\frac{\mathbf{238U}_{spk} + \mathbf{238U}_{norm} + \mathbf{238U}_{exdef}}{\mathbf{233}U_{spk}}\right)_{t}}{\left(\frac{238\mathrm{U}}{233\mathrm{U}}\right)_{m}}\right] - 1}{5} = \frac{\left[\frac{\left(\frac{\mathbf{233U}_{spk}}{\mathbf{238U}_{norm}/137.88 + \mathbf{235}U_{spk}}\right)}{\left(\frac{233\mathrm{U}}{235\mathrm{U}}\right)_{m}}\right] - 1}{-2}$$

Eq.7a

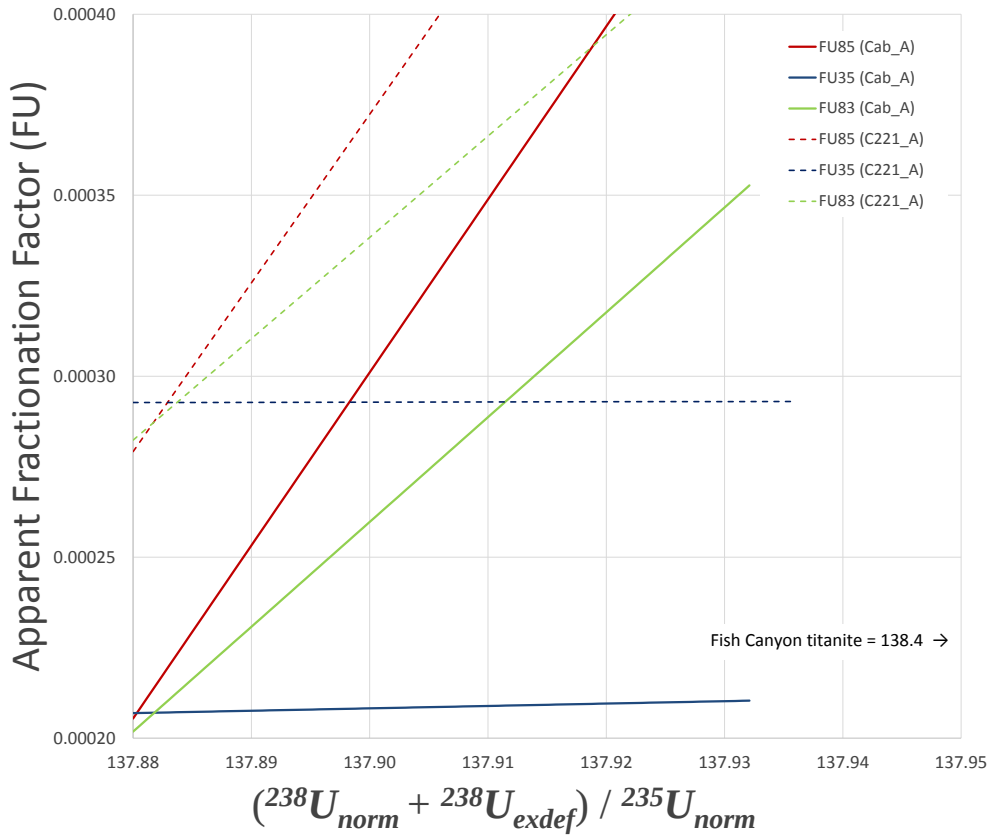

Figure 5 Graphical representation of Isotope Ratio Triangulation. Fractionation factors (FU) calculated from two samples at the extremes of U concentration using varying molar abundance of excess ^{238}U (plot generated from only positive values of $^{238}\mathbf{U}_{exdef}$) and for varying amounts of ^{238}U due to potential uncertainty in the molar abundance of ^{238}U as a result of the use of equation 5 as a starting point for varying $^{238}\mathbf{U}_{norm}$. Dashed lines are sample C221, fraction A, solid lines are sample Cabarrus, fraction A (see Appendix A). The two samples show very different fractionation factors (intersections) of about 0.00022/AMU for Cabarrus_A and about 0.00076 for C221_A due to differences in mass spectrometry run conditions (temperature, matrix effects, etc.). However, intersections occur very close to ^{238}U/^{235}U = 137.88 indicating very minor or unresolvable ^{238}U/^{235}U anomaly in these two samples.

Quantitative Solution

The graphical representation of this solution demonstrates the efficacy of this method. A quantitative solution is achieved by determining the equation of each line:

$$y_{85} = m_{85}x_{85} + b_{85}$$

Eq.8

$$y_{35} = m_{35}x_{35} + b_{35}$$

Eq.9

$$y_{83} = m_{83}x_{83} + b_{83}$$

Eq.10

Where;

$$y = FU\ (Eq.4a, Eq.4b, or\ Eq.4c)$$

$$x = \frac{(238\mathrm{U}_{norm} + 238\mathrm{U}_{exdef})}{(238\mathrm{U}_{norm})}$$

$$m = \frac{(y_2 - y_1)}{(x_2 - x_1)}$$

$$b = y - mx$$

and then setting them equal to each other to determine the congruous x and y points, or the point of intersection:

FU85=FU35:

$$x_{intersect} = \frac{b_{35} - b_{85}}{m_{85} - m_{35}}$$

Eq.11a

$$y_{intersect} = m_{85}x_{intersect} + b_{85}$$

Eq. 11b

FU85=FU83:

$$x_{intersect} = \frac{b_{83} - b_{85}}{m_{85} - m_{83}}$$

Eq. 12a

$$y_{intersect} = m_{85}x_{intersect} + b_{85}$$

Eq. 12b

FU83=FU35:

$$x_{intersect} = \frac{b_{35} - b_{83}}{m_{83} - m_{35}}$$

Eq. 13a

$$y_{intersect} = m_{83}x_{intersect} + b_{83}$$

Eq. 13b

The intersection, or near intersection, of all three points is where all three fractionation factors are in agreement; representing the true, fractionation corrected, $^{238}U/^{235}U$ value.

Error Propagation

The ability of the above method to resolve anomalous $^{238}U/^{235}U$ ratios on the order of that of the Fish Canyon tuff titanite (Heiss et al., 2012) depends on measurement precision and spike isotopic composition and concentrations being precise enough to resolve $^{238}U_{exdef}$ to better than about 1000 ppm. Error was propagated through the above equations and factors in error from all measured ratios (RU85m, RU35m and RU83m) as well as uncertainty in spike concentration and isotope ratios. Error was calculated through quadrature as outlined in (Schmitz and Schoene 2007). Figure 6 demonstrates the ability to resolve differences with the necessary precision.

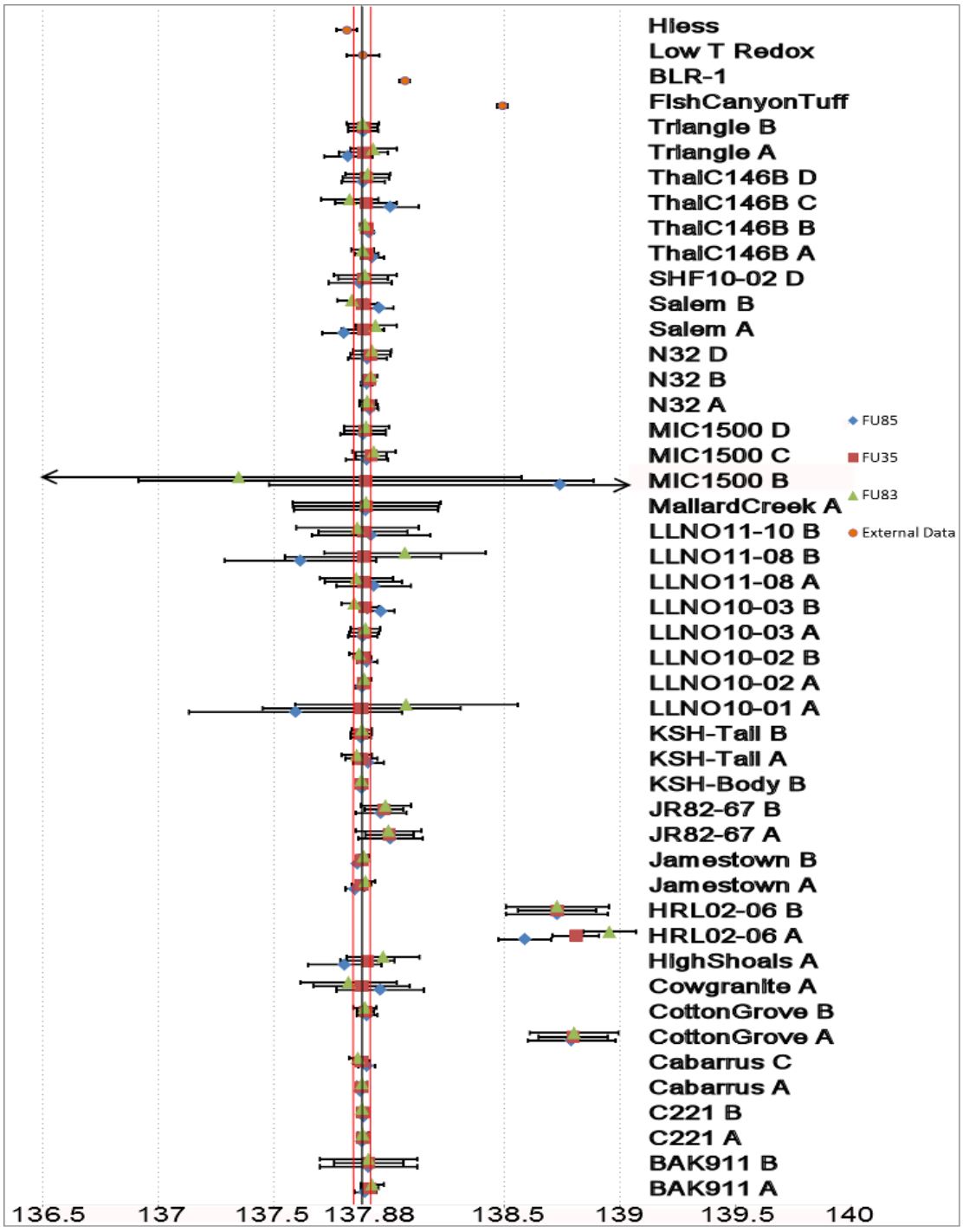

Figure 6 $^{238}U/^{235}U$ ratio of all samples as determined using the IRT method. Note that CottonGrove A and both HRL02-06 samples were the only samples that did not fall within error of $^{238}U/^{235}U = 137.88$. The weighted average of all but those three is 137.89 ± .02, represented by the red lines.

RESULTS

Ages

A total of 43 titanite aliquots (Fig. 7) were analyzed from 24 rock samples from a variety of locations and geologic settings. Of these, 20 samples successfully yielded usable U-Pb pairs which were used to determine $^{207}Pb/^{206}Pb$, $^{207}Pb/^{235}U$, $^{206}Pb/^{238}Pb$ ages ranging from 250 Ma to over 2.5 Ga (Appendix A). Samples C221 B, HLR02-06 A, and HLR02-06 B all yielded very poor Pb data due to inadequate Pb abundance. Discordance was observed in several samples, most notably CottonGrove B, but most sample ages were in close internal agreement with one another when reliable U-Pb fractions were effectively measured for each.

$^{238}U/^{235}U$

$^{238}U/^{235}U$ ratios were computed for 43 aliquots using the IRT method. Of these 43 aliquots, 40 ratios were within error of the accepted $^{238}U/^{235}U$ value of 137.88. Three aliquots fell noticeably outside of this "natural" uranium value. These aliquots were CottonGrove A, HLR02-06 A, and HLR02-06 B which average $^{238}U/^{235}U$ values of 138.80 ± 0.17 (2σ), 138.78 ± 0.11 (2σ) and 138.73 ± 0.21 (2σ), respectively. Excluding these three aliquots, the samples yielded a weighted average $^{238}U/^{235}U$ value of 137.89 ± 0.02 (2σ). It is worth noting that two samples, although strictly within error of 137.88, suggest a slight positive anomaly; JR82-67 A and JR82-67 B yielded average values of

138.00 ± 0.12 (2σ) and 137.98 ± 0.10 (2σ).

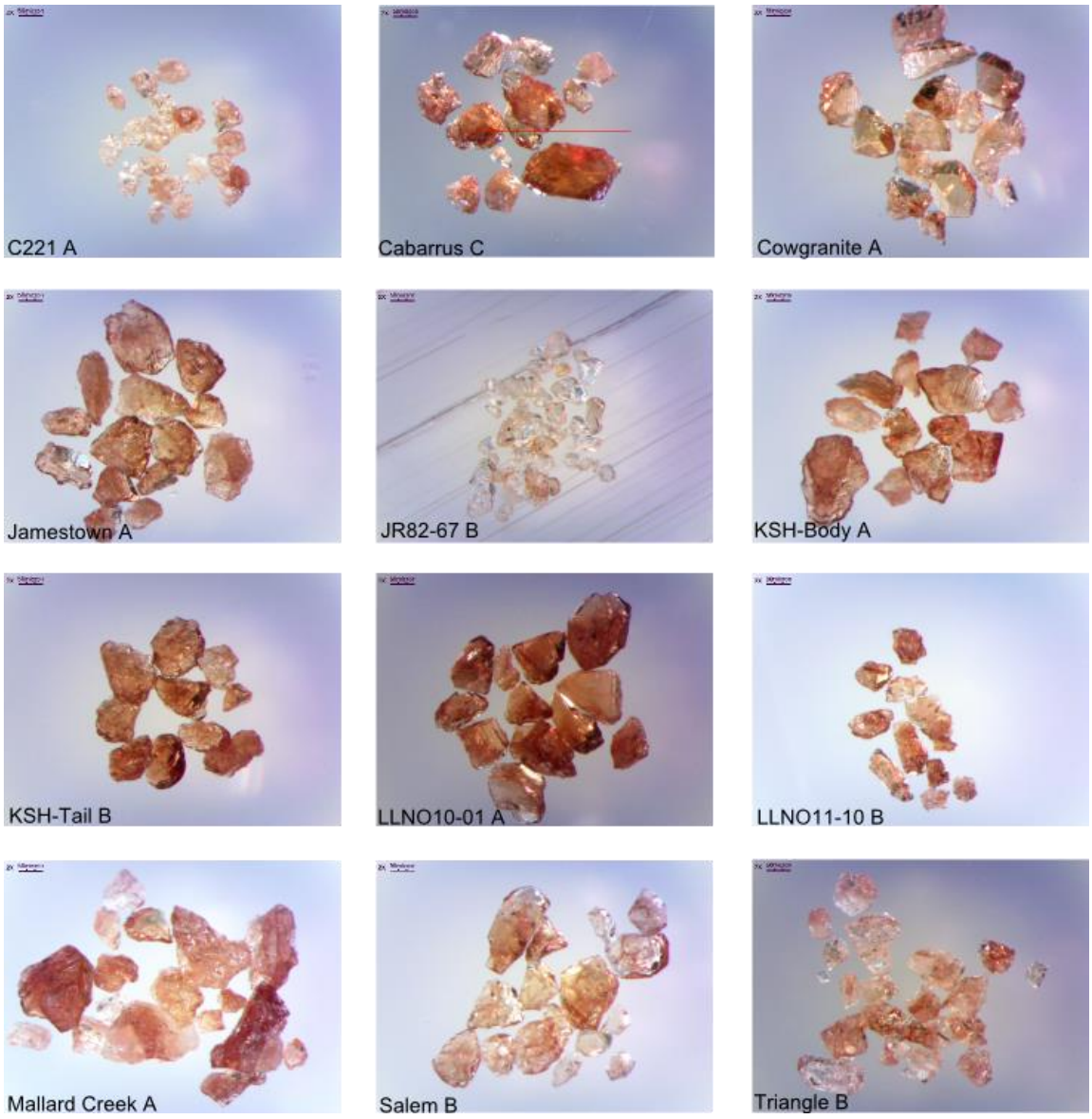

Figure 7 Photomicrographs of twelve example titanite aliquots. Scale bars in top left are 50 microns.

DISCUSSION

The $^{238}U/^{235}U$ ratio was effectively determined for all 43 aliquots with the precision necessary to resolve any deviation from the accepted value of 137.88 greater than about 200 ppm. Excluding the three outliers discussed in the previous section, these samples had an average measured value of 137.89 ± 0.02 (2σ). This value overlaps at the extremes of uncertainty (Fig. 6) with the proposed new value of 137.818 by Hiess et al. (2012), however, the data consistently trend towards the previous value of 137.88, as proposed by (Jaffey et al. 1971).

Samples that showed wide margins of error like Mallard Creek, LLNO11-10 B, LLNO11-08 B, Cow Granite A, and High Shoals A all produced very low uranium signals ranging from 0.002 mV to 0.0004 mV. Poor counting statistics from such low signals are the likely cause of such a wide error margin. Aliquots which showed discordance and wide margins of error, like MIC1500 B, LLNO11-08 B, and LLNO10-01 A all ran at unusually high currents, over 3200 mA. IRT is dependent on the linear fractionation law model and is effective for normal running conditions of ID-TIMS analyses; however, this model fails at unusually high running temperatures, resulting from such high currents, as the total fractionation gradually exceeds the 0.1% threshold. The discordance documented MIC1500 B, LLNO11-08 B, and LLNO10-01are the result of model failing as linear fractionation law no longer applies. However, it is worth

noting that when the average was taken all aliquots measured very near the accepted $^{238}U/^{235}U$ value of 137.88.

Brennecka et al. (2010) noted that uranium deposited in low temperature redox environments was consistently 0.4‰ higher than its high temperature deposition and non-redox counterparts. Brennecka et al. (2010) also noted that the ThermoFinnigan Neptune yielded slightly lower $^{238}U/^{235}U$ ratios, less than 0.01‰, than the Thermo Triton when testing natural uranium standard CRM129-A; thereby demonstrating that instrumental bias can play a role, though barely measureable. It is unlikely that either low temperature redox or instrumental bias is causing the deviation seen in the three major outliers of this study. A more likely explanation is that the uranium was lost during sample processing and all three record lab uranium blank composition. The uranium concentration in all three major outliers is anomalously low, roughly 75 pg of uranium each, compared to tens or hundreds of nanograms in other samples. This amount of blank is significantly greater than ever measured directly and is notably of higher $^{238}U/^{235}U$ (depleted U). This would render the data for these three samples irrelevant for the purposes of exploring uranium isotope fractionation in titanite. It does, however, demonstrate that the IRT method is effective at resolving minor differences in $^{238}U/^{235}U$ ratios and that uranium blank is depleted in ^{235}U much like manmade depleted uranium, though not to the same degree.

The only other samples which yielded any sign of potentially anomalous $^{238}U/^{235}U$ values were JR82-67 A and JR82-67 B, both from a late Archean trondhjemite in the Dharwar craton of western India. The titanite U-Pb ages are about 2.5 Ga (Appendix A). This age coincides with the late Archean to early Proterozoic "Great Oxidation Event" (Murakami et al. 2001). Kendall et al. (2013) observed anomalously low $^{238}U/^{235}U$ values in black shales deposited during this time. Brennecka et al. (2008) demonstrated that uranium will fractionate when adsorbing onto Mn oxyhydroxide due to a difference in coordination environment, which is believed to have been taking place as the world's oceans became oxygenated creating ferro-manganese sediments enriched in ^{235}U by up to 0.2‰ (Brennecka et al. 2011). If this is the case, the isotopically heavy reservoir would have been seawater. Because sample JR82-67 is from an Archean subduction-related pluton, it is possible that this seawater fluxed the hotter, shallower Archean mantle wedge to cause melting and that the uranium in this water was somehow incorporated into the final differentiated magmas to become incorporated into titanite. Further study is necessary to test this hypothesis.

This study clearly demonstrates the IRT method's ability to resolve uranium isotope ratio variations at the same level, like those seen in JR82-67 A, JR82-67 B, Cotton Grove A, HLR02-06 A, and HLR02-06 B, without the use of the ^{236}U-^{233}U spike. The IRT method of determining isotopic ratios allows U-Pb data already collected using the $^{235}U/^{233}U$ spike to be scanned easily for potentially anomalous $^{238}U/^{235}U$ values. By redefining the input variables, this method could also be applied to other elements measured with a double spike in which the spike shares one of the isotopes of interest.

CONCLUSIONS

Isotope Ratio Triangulation is a new tool for rapidly evaluating the potential for $^{238}U/^{235}U$ anomalies in samples spiked with a ^{235}U-^{233}U spike. With IRT, large existing geochronologic data sets can be evaluated and the geologic causes and geochronologic consequences of variations in uranium isotope ratios can be explored more fully. This study demonstrates this method's ability to resolve permil variations in $^{238}U/^{235}U$ ratios like those observed in Brennecka et al. (2010), Hiess et al. (2012) and Kendall et al. (2013).

In addition, this study demonstrates that, if laboratory blank is the source of low-U samples (CottonGrove A, HLR02-06 A, and HLR02-06 B), then that uranium is not entirely of natural composition; it must contain some component of depleted uranium. The composition of the U blank should thus be taken into account in high-precision geochronology.

Lastly, titanite from sample JR82-67 yield only very slightly higher $^{238}U/^{235}U$ values which coincided with the Archean and Proterozoic oceanic oxidation. Oceanic oxidation may result in several hundred permil variation due to redox sensitivity of atomic mass (Kendall et al. 2013, Brennecka et al. 2008). The geochemical and petrogenetic circumstances that resulted in incorporation of this uranium into titanite remain to be resolved.

REFERENCES

Brennecka, G. A., L. E. Borg, I. D. Hutcheon, M. A. Sharp, and A. D. Anbar. 2010. "Natural variations in uranium isotope ratios of uranium ore concentrates: Understanding the U-238/U-235 fractionation mechanism." *Earth and Planetary Science Letters* 291 (1-4):228-233. doi: DOI 10.1016/j.epsl.2010.01.023.

Brennecka, G. A., L. E. Wasylenki, J. R. Bargar, S. Weyer, and A. D. Anbar. 2011. "Uranium Isotope Fractionation during Adsorption to Mn-Oxyhydroxides." *Environmental Science & Technology* 45 (4):1370-1375. doi: Doi 10.1021/Es103061v.

Brennecka, G. A., L. E. Wasylenki, S. Weyer, and A. D. Anbar. 2008. "Experiments demonstrate that Uranium isotopes fractionate during adsorption to Mn-oxides." *Geochimica Et Cosmochimica Acta* 72 (12):A114-A114.

Condon, D. J., N. McLean, S. R. Noble, and S. A. Bowring. 2010. "Isotopic composition (U-238/U-235) of some commonly used uranium reference materials." *Geochimica Et Cosmochimica Acta* 74 (24):7127-7143. doi: DOI 10.1016/j.gca.2010.09.019.

Cowan, G. A., and H. H. Adler. 1976. "Variability of Natural Abundance of U-235." *Geochimica Et Cosmochimica Acta* 40 (12):1487-1490. doi: Doi 10.1016/0016-7037(76)90087-9.

Hiess, J., D. J. Condon, N. McLean, and S. R. Noble. 2012. "U-238/U-235 Systematics in Terrestrial Uranium-Bearing Minerals." *Science* 335 (6076):1610-1614. doi: DOI 10.1126/science.1215507.

Jaffey, A. H., K. F. Flynn, Glendeni.Le, W. C. Bentley, and A. M. Essling. 1971. "Precision Measurement of Half-Lives and Specific Activities of U-235 and U-238." *Physical Review C* 4 (5):1889-&. doi: DOI 10.1103/PhysRevC.4.1889.

Kendall, B., G. A. Brennecka, S. Weyer, and A. D. Anbar. 2013. "Uranium isotope fractionation suggests oxidative uranium mobilization at 2.50 Ga." *Chemical Geology* 362:105-114. doi: DOI 10.1016/j.chemgeo.2013.08.010.

Kylander-Clark, A. R. C., B. R. Hacker, and J. M. Mattinson. 2008. "Slow exhumation of UHP terranes: Titanite and rutile ages of the Western Gneiss Region, Norway." *Earth and Planetary Science Letters* 272 (3-4):531-540. doi: DOI 10.1016/j.epsl.2008.05.019.

Le Bas, MJ, RW Le Maitre, Arthur Streckeisen, and Bruno Zanettin. 1986. "A chemical classification of volcanic rocks based on the total alkali-silica diagram." *Journal of petrology* 27 (3):745-750.

Lipman, P., M. Dungan, and O. Bachmann. 1997. "Comagmatic granophyric granite in the Fish Canyon Tuff, Colorado: Implications for magma-chamber processes during a large ash-flow eruption." *Geology* 25 (10):915-918. doi: Doi 10.1130/0091-7613(1997)025<0915:Cggitf>2.3.Co;2.

Mattinson, J. M. 2005a. "U-Pb inter-laboratory calibrations using zircon samples: Application of the new CA-TIMS technique." *Geochimica Et Cosmochimica Acta* 69 (10):A319-A319.

Mattinson, J. M. 2005b. "Zircon U-Pb chemical abrasion ("CA-TIMS") method: Combined annealing and multi-step partial dissolution analysis for improved precision and accuracy of zircon ages." *Chemical Geology* 220 (1-2):47-66. doi: DOI 10.1016/j.chemgeo.2005.03.011.

Mattinson, J. M. 2010. "Analysis of the relative decay constants of U-235 and U-238 by multi-step CA-TIMS measurements of closed-system natural zircon samples." *Chemical Geology* 275 (3-4):186-198. doi: DOI 10.1016/j.chemgeo.2010.05.007.

Mattinson, J.M. 1972. "Preparation of Hydrofluoric, Hydrochloric, and Nitric Acids at Ultralow Lead Levels." *Analytical Chemistry* 44 (9):1715-&. doi: Doi 10.1021/Ac60317a032.

McLean, N. M., J. F. Bowring, and S. A. Bowring. 2011. "An algorithm for U-Pb isotope dilution data reduction and uncertainty propagation." *Geochemistry Geophysics Geosystems* 12. doi: Artn Q0aa18 Doi 10.1029/2010gc003478.

Murakami, Takashi, Satoshi Utsunomiya, Yoji Imazu, and Nirankar Prasad. 2001. "Direct evidence of late Archean to early Proterozoic anoxic atmosphere from a product of 2.5 Ga old weathering." *Earth and Planetary Science Letters* 184 (2):523-528.

Nielsen, S. G., M. Rehkamper, M. D. Norman, A. N. Halliday, and D. Harrison. 2006. "Thallium isotopic evidence for ferromanganese sediments in the mantle source of Hawaiian basalts." *Nature* 439 (7074):314-317. doi: Doi 10.1038/Nature04450.

Nielsen, S. G., M. Rehkamper, D. Porcelli, P. Andersson, A. N. Halliday, P. W. Swarzenski, C. Latkoczy, and D. Gunther. 2005. "Thallium isotope composition of the upper continental crust and rivers - An investigation of the continental sources of dissolved marine thallium." *Geochimica Et Cosmochimica Acta* 69 (8):2007-2019. doi: DOI 10.1016/j.gca.2004.10.025.

Schauble, E. A. 2007. "Role of nuclear volume in driving equilibrium stable isotope fractionation of mercury, thallium, and other very heavy elements." *Geochimica Et Cosmochimica Acta* 71 (9):2170-2189. doi: DOI 10.1016/j.gca.2007.02.004.

Schmitz, M. D., and B. Schoene. 2007. "Derivation of isotope ratios, errors, and error correlations for U-Pb geochronology using Pb-205-U-235-(U-233)-spiked isotope dilution thermal ionization mass spectrometric data." *Geochemistry Geophysics Geosystems* 8. doi: Artn Q08006 Doi 10.1029/2006gc001492.

Schoene, B., J. L. Crowley, D. J. Condon, M. D. Schmitz, and S. A. Bowring. 2006. "Reassessing the uranium decay constants for geochronology using ID-TIMS U-Pb data." *Geochimica Et Cosmochimica Acta* 70 (2):426-445. doi: DOI 10.1016/j.gca.2005.09.007.

Scott, D. J., and M. R. S. Onge. 1995. "Constraints on Pb Closure Temperature in Titanite Based on Rocks from the Ungava Orogen, Canada - Implications for U-Pb Geochronology and P-T-T Path Determinations." *Geology* 23 (12):1123-1126. doi: Doi 10.1130/0091-7613(1995)023<1123:Copcti>2.3.Co;2.

Smith, C. N., S. E. Kesler, B. Klaue, and J. D. Blum. 2005. "Mercury isotope fractionation in fossil hydrothermal systems." *Geology* 33 (10):825-828. doi: Doi 10.1130/G21863.1.

Steiger, R. H., and E. Jager. 1977. "Subcommission on Geochronology - Convention on Use of Decay Constants in Geochronology and Cosmochronology." *Earth and Planetary Science Letters* 36 (3):359-362. doi: Doi 10.1016/0012-821x(77)90060-7.

Stirling, C. H., M. B. Andersen, E. K. Potter, and A. N. Halliday. 2007. "Low-temperature isotopic fractionation of uranium." *Earth and Planetary Science Letters* 264 (1-2):208-225. doi: DOI 10.1016/j.epsl.2007.09.019.

Stirling, C. H., M. B. Andersen, R. Warthmann, and A. N. Halliday. 2007. "Isotopic fractionation of uranium in low-temperature environments." *Geochimica Et Cosmochimica Acta* 71 (15):A975-A975.

Tilton, G. R. 1968. "Model Lead Ages and Age of Earth." *Transactions-American Geophysical Union* 49 (1):349-&.

Tucker, R. D., P. Robinson, A. Solli, D. G. Gee, T. Thorsnes, T. E. Krogh, O. Nordgulen, and M. E. Bickford. 2004. "Thrusting and extension in the scandian hinterland, Norway: New U-Pb ages and tectonostratigraphic evidence." *American Journal of Science* 304 (6):477-532. doi: DOI 10.2475/ajs.304.6.477.

Whitney, J. A., and J. C. Stormer. 1985. "Mineralogy, Petrology, and Magmatic Conditions from the Fish-Canyon Tuff, Central San-Juan Volcanic Field, Colorado." *Journal of Petrology* 26 (3):726-762.

Young, Edward D, Albert Galy, and Hiroko Nagahara. 2002. "Kinetic and equilibrium mass-dependent isotope fractionation laws in nature and their geochemical and cosmochemical significance." *Geochimica et Cosmochimica Acta* 66 (6):1095-1104.

APPENDIX A

			BAK911_A	BAK911_B	C221_A	C221_B	Cabarrus_A	Cabarrus_C	CottonGrove_A	CottonGrove_B	Cowgranite_A
	Spike weight	(b)	0.102	0.102	0.102	0.102	0.075	0.075	0.102	0.102	0.090
Compositional	U ppm	(c)	1829.531	1963.391	11834.883	10237.794	109081.496	49690.113	75.613	3232.123	189609.678
Parameters	Th/U	(d)	0.133	0.206	0.849	0.252	2.319	4.245	0.794	0.597	7.215
	Pb ppm	(c)	441.594	461.634	1639.278	35581.741	11709.703	7295.899	187.492	323.751	41626.730
	206Pb* x 10-13 mol	(e)	4.949	5.088	39.466	14.459	302.408	137.213	0.220	6.403	362.742
	mol% 206Pb*	(e)	0.553	0.550	0.853	0.033	0.978	0.958	0.092	0.771	0.650
	Pb*/Pbc	(e)	0.339	0.343	1.929	0.012	20.344	13.713	0.043	1.061	1.577
	Pbc (pg)	(e)	329.710	343.714	559.790	35147.167	548.670	495.950	179.779	157.111	16154.768
	206Pb/204Pb	(f)	41.187	40.869	125.439	19.017	855.240	438.462	20.258	80.272	52.486
Radiogenic	208Pb/206Pb	(g)	0.042	0.068	0.268	0.261	0.729	1.338	0.541	0.204	2.333
Isotope Ratios	207Pb/206Pb	(g)	0.055	0.057	0.058	0.209	0.055	0.055	0.156	0.057	0.053
	% err	(h)	10.149	7.549	0.656	59.075		0.210	431.883	2.632	2.776
	207Pb/235U	(g)	0.493	0.489	0.635	0.975	0.505	0.504	1.508	0.375	0.338
	% err	(h)	10.145	7.534	0.616	42.194	0.034	0.243	432.010	2.626	2.762
	206Pb/238U	(g)	0.065	0.062	0.080	0.034	0.066	0.066	0.070	0.048	0.046
	% err	(h)	1.335	1.366	0.279	47.871	0.059	0.145	16.896	0.501	0.914
	coef.		0.063	0.080	0.076	0.144		0.515	0.027	0.083	0.151
Isotopic Ages	207Pb/206Pb	(i)	415.654	495.766	514.570	2895.438	417.370	420.550	2418.126	501.881	347.164
	±	(h)	226.750	166.338	14.414	958.183		4.680	7330.030	57.940	62.784
	207Pb/235U	(i)	406.781	404.454	499.247	690.896	415.245	414.327	933.625	323.463	295.451
	±	(h)	34.004	25.133	2.428	211.471	0.117	0.828	2637.524	7.275	7.082
	206Pb/238U	(i)	405.220	388.645	495.911	214.750	414.862	413.211	435.477	299.218	288.949
	±	(h)	5.240	5.151	1.332	101.074	0.236	0.581	71.139	1.464	2.583
Raw Data	206Pb/204Pb Mean	(j)	40.915	40.606	124.804	18.975	851.453	436.424	20.075	79.303	52.328
	% Standard Error	(h)	0.138	0.131	0.058	0.141	0.053	0.093	0.300	0.123	0.122
	206Pb/207Pb Mean	(j)	2.443	2.420	5.763	1.209	13.864	11.310	1.275	4.188	3.013
	% Standard Error	(h)	0.261	0.187	0.057	0.028	0.018	0.082	0.421	0.246	0.143
	206Pb/205Pb Mean	(j)	0.312	0.323	1.614	15.362	14.667	6.797	0.084	0.290	2.209
	% Standard Error	(h)	0.094	0.067	0.020	0.105	0.020	0.057	0.290	0.063	0.098
	207Pb/205Pb Mean	(j)	0.128	0.134	0.280	12.706	1.058	0.601	0.066	0.069	0.733
	% Standard Error	(h)	0.236	0.178	0.062	0.111	0.027	0.093	0.310	0.243	0.155
	204Pb/205Pb Mean	(j)	0.007	0.007	0.011	0.716	0.016	0.014	0.003	0.003	0.038
	% Standard Error	(h)	0.109	0.091	0.062	0.131	0.105	0.102	0.159	0.112	0.174
	208Pb/205Pb Mean	(h)	0.297	0.314	0.859	30.972	11.100	9.283	0.162	0.184	4.947
	% Standard Error	(h)	0.099	0.078	0.026	0.113	0.020	0.057	0.123	0.112	0.107
	202Pb/205Pb Mean	(j)	1.100	1.100	1.100	1.100	1.100	1.100	1.100	1.100	1.100
	% Standard Error	(h)	0.100	0.100	0.100	0.100	0.100	0.100	0.100	0.100	0.100
	238U/235U Mean	(j)	0.039	0.042	0.211	0.184	2.517	1.160	0.009	0.063	0.379
	% Standard Error	(h)	0.022	0.107	0.008	0.007	0.006	0.013	0.087	0.019	0.089
	233U/235U Mean	(j)	1.035	1.033	1.033	1.034	1.016	1.027	1.035	1.036	1.029
	% Standard Error	(h)	0.003	0.008	0.004	0.002	0.008	0.013	0.003	0.008	0.035
	238U/233U Mean	(j)	0.038	0.040	0.204	0.178	2.478	1.129	0.009	0.061	0.368
	% Standard Error	(h)	0.023	0.107	0.011	0.007	0.007	0.015	0.087	0.025	0.109

(a) labels for fractions composed of a cluster of titanite grains or fragments.

(b) Weight of 535 double spike added to each fraction

(c) Nominal U and total Pb concentrations subject to uncertainty in photomicrographic estimation of weight and partial dissolution during chemical abrasion.

(d) Model Th/U ratio calculated from radiogenic 208Pb/206Pb ratio and 207Pb/235U age.

(e) Pb* and Pbc represent radiogenic and common Pb, respectively; mol % ^{206}Pb* with respect to radiogenic, blank and initial common Pb.

(f) Measured ratio corrected for spike and fractionation only.

(g) Corrected for fractionation, spike, and common Pb; up to 1 pg of common Pb was assumed to be procedural blank: 206Pb/204Pb = 18.60 ± 0.80%; 207Pb/204Pb = 15.69 ± 0.32%; 208Pb/204Pb = 38.51 ± 0.74% (all uncertainties 1-sigma). Excess over blank was assigned to initial common Pb.

(h) Errors are 2-sigma, propagated using the algorithms of Schmitz and Schoene (2007) and Crowley et al. (2007).

(i) Calculations are based on the decay constants of Jaffey et al. (1971). 206Pb/238U and 207Pb/206Pb ages corrected for initial disequilibrium in 230Th/238U using Th/U [magma] = 3.

(j) Data which has been selected through Tripoli and subjected to a 2-sigma filter, but which has not been corrected for fractionation, spike, or Pb.

Table A1 Samples: BAK 911, C221, Cabarrus, CottonGrove and Cowgranite. Raw and processed data used for calculations.

			HighShoals_A	HRL02-06_A	HRL02-06_B	Jamestown_A	Jamestown_B	JR82-67_A	JR82-67_B	KSH-Body_B	KSH-Tail _A
Compositional	Spike weight	(b)	0.020	0.102	0.102	0.075	0.075	0.075	0.075	0.075	0.075
Parameters	U ppm	(c)	2289.995	74.769	81.236	113545.392	97050.209	525.850	651.131	166987.534	131177.790
	Th/U	(d)	0.549	0.986		0.352	0.355	0.931	0.965	0.062	0.944
	Pb ppm	(c)	383.215	77.270	192.921	11547.287	10031.717	672.798	805.112	11519.529	13695.805
	206Pb* x 10-13 mol	(e)	3.597	0.192	0.291	459.412	390.095	10.307	13.927	468.828	388.865
	mol% 206Pb*	(e)	0.504	0.175	0.114	0.988	0.981	0.697	0.744	0.971	0.919
	Pb*/Pbc	(e)	0.314	0.038	0.029	23.709	15.262	0.823	1.040	9.136	3.831
	Pbc (pg)	(e)	291.660	74.476	187.426	467.393	616.958	369.164	394.698	1136.663	2835.391
	206Pb/204Pb	(f)	37.122	22.315	20.753	1510.779	978.413	60.784	71.968	644.651	226.631
Radiogenic	208Pb/206Pb	(g)	0.181	-0.256	0.260	0.110	0.111	0.262	0.260	0.019	0.297
Isotope Ratios	207Pb/206Pb	(g)	0.053	-0.032	-0.340	0.060	0.060	0.165	0.168	0.055	0.056
	% err	(h)	3.996	4345.282	876.607	0.047	0.071	0.851	0.673	0.122	0.688
	207Pb/235U	(g)	0.276	-0.273	-4.022	0.801	0.795	10.683	11.875	0.514	0.548
	% err	(h)	3.749	4344.976	874.147	0.088	0.090	0.588	0.454	0.135	0.795
	206Pb/238U	(g)	0.038	0.062	0.086	0.097	0.096	0.470	0.513	0.067	0.071
	% err	(h)	1.573	10.917	31.366	0.070	0.057	0.729	0.575	0.076	0.419
	coef.		0.048	-0.027	-0.061	0.848	0.615	0.178	0.162	0.444	0.501
Isotopic Ages	207Pb/206Pb	(i)	335.752	-4999.998	-4999.998	598.194	596.123	2506.334	2537.232	425.038	448.723
	±	(h)	90.552	836779.690	1783684.628	1.014	1.541	14.312	11.281	2.714	15.292
	207Pb/235U	(i)	247.625	-323.557		597.193	593.797	2495.978	2594.571	420.816	443.663
	±	(h)	8.239	-16556.543	11812.939	0.398	0.406	5.457	4.251	0.464	2.858
	206Pb/238U	(i)	238.424	385.108	530.998	596.929	593.188	2483.271	2668.646	420.046	442.688
	±	(h)	3.682	40.798	159.856	0.402	0.326	15.017	12.569	0.308	1.791
Raw Data	206Pb/204Pb Mean	(j)	37.005	21.891	20.570	1503.496	974.321	60.466	71.602	642.541	226.037
	% Standard Error	(h)	0.055	0.723	1.643	0.057	0.046	0.052	0.047	0.042	0.197
	206Pb/207Pb Mean	(j)	2.237	1.441	1.402	14.410	13.412	2.691	2.927	12.838	8.323
	% Standard Error	(h)	0.050	0.970	2.945	0.012	0.015	0.060	0.049	0.014	0.047
	206Pb/205Pb Mean	(j)	1.269	0.038	0.090	22.072	18.868	0.702	0.888	22.903	20.085
	% Standard Error	(h)	0.032	0.668	1.585	0.019	0.019	0.026	0.024	0.025	0.186
	207Pb/205Pb Mean	(j)	0.567	0.027	0.066	1.532	1.407	0.261	0.304	1.784	2.414
	% Standard Error	(h)	0.046	0.877	2.017	0.024	0.022	0.054	0.051	0.027	0.174
	204Pb/205Pb Mean	(j)	0.032	0.002	0.004	0.013	0.018	0.010	0.011	0.033	0.083
	% Standard Error	(h)	0.047	0.219	0.413	0.067	0.055	0.081	0.056	0.042	0.225
	208Pb/205Pb Mean	(h)	1.421	0.064	0.167	2.944	2.779	0.569	0.643	1.788	8.851
	% Standard Error	(h)	0.032	0.317	0.860	0.021	0.021	0.028	0.027	0.027	0.179
	202Pb/205Pb Mean	(j)	1.100	1.100	1.100	1.100	1.100	1.100	1.100	1.100	1.100
	% Standard Error	(h)	0.100	0.100	0.100	0.100	0.100	0.100	0.100	0.100	0.100
	238U/235U Mean	(j)	0.208	0.009	0.009	2.613	2.241	0.020	0.023	3.805	3.009
	% Standard Error	(h)	0.079	0.037	0.104	0.013	0.005	0.068	0.053	0.004	0.020
	233U/235U Mean	(j)	1.034	1.035	1.034	1.016	1.019	1.035	1.035	1.007	1.013
	% Standard Error	(h)	0.017	0.004	0.009	0.014	0.006	0.004	0.004	0.005	0.024
	238U/233U Mean	(j)	0.202	0.009	0.009	2.571	2.199	0.019	0.022	3.778	2.969
	% Standard Error	(h)	0.078	0.039	0.106	0.015	0.005	0.070	0.053	0.004	0.017

(a) labels for fractions composed of a cluster of titanite grains or fragments.

(b) Weight of 535 double spike added to each fraction

(c) Nominal U and total Pb concentrations subject to uncertainty in photomicrographic estimation of weight and partial dissolution during chemical abrasion.

(d) Model Th/U ratio calculated from radiogenic 208Pb/206Pb ratio and 207Pb/235U age.

(e) Pb* and Pbc represent radiogenic and common Pb, respectively; mol % ^{206}Pb* with respect to radiogenic, blank and initial common Pb.

(f) Measured ratio corrected for spike and fractionation only.

(g) Corrected for fractionation, spike, and common Pb; up to 1 pg of common Pb was assumed to be procedural blank: 206Pb/204Pb = 18.60 ± 0.80%; 207Pb/204Pb = 15.69 ± 0.32%; 208Pb/204Pb = 38.51 ± 0.74% (all uncertainties 1-sigma). Excess over blank was assigned to initial common Pb.

(h) Errors are 2-sigma, propagated using the algorithms of Schmitz and Schoene (2007) and Crowley et al. (2007).

(i) Calculations are based on the decay constants of Jaffey et al. (1971). 206Pb/238U and 207Pb/206Pb ages corrected for initial disequilibrium in 230Th/238U using Th/U [magma] = 3.

(j) Data which has been selected through Tripoli and subjected to a 2-sigma filter, but which has not been corrected for fractionation, spike, or Pb.

Table A1 Continued Samples: High Shoals, HLR02-06, Jamestown, JR82-07, KSH Body and KSH Tail. Raw and processed data used for calculations.

		(a)	KSH-Tail_B	LLNO10-01_A	LLNO10-02_A	LLNO10-02_B	LLNO10-03_A	LLNO10-03_B	LLNO11-08_A	LLNO11-08_B	LLN011-10_B
Compositional	Spike weight	(b)	0.075	0.102	0.102	0.102	0.020	0.020	0.090	0.090	0.102
Parameters	U ppm	(c)	125456.071	37066.432	7122.670	30232.869	22021.467	30770.288	78999.380	65809.326	9709.653
	Th/U	(d)	0.987	0.961	32.282	0.873	0.571	0.479	1.399	1.431	1.071
	Pb ppm	(c)	13446.329	11212.514	16273.756	7614.810	4929.915	6409.711	32009.466	25256.247	2638.553
	206Pb* x 10-13 mol	(e)	369.386	291.465	43.522	233.516	169.377	236.683	714.940	511.637	59.486
	mol% 206Pb*	(e)	0.910	0.888	0.391	0.943	0.961	0.978	0.852	0.819	0.847
	Pb*/Pbc	(e)	3.440	2.706	1.909	5.519	7.718	13.290	2.114	1.710	1.985
	Pbc (pg)	(e)	3028.603	3025.768	5595.442	1168.176	565.542	448.612	10280.621	9321.004	884.046
	206Pb/204Pb	(f)	203.581	164.653	30.203	321.907	473.123	819.437	123.984	101.737	120.561
Radiogenic	208Pb/206Pb	(g)	0.310	0.286	10.731	0.262	0.173	0.145	0.396	0.432	0.352
Isotope Ratios	207Pb/206Pb	(g)	0.056	0.075	0.077	0.075	0.076	0.076	0.075	0.076	0.076
	% err	(h)	0.321	0.429	4.398	0.419	0.229	0.132	0.119	0.446	0.529
	207Pb/235U	(g)	0.543	1.940	1.560	1.917	1.931	1.928	2.251	1.949	1.540
	% err	(h)	0.309	0.711	3.674	0.559	0.354	0.271	0.355	0.577	0.543
	206Pb/238U	(g)	0.071	0.189	0.146	0.185	0.184	0.184	0.217	0.186	0.147
	% err	(h)	0.177	0.613	2.488	0.395	0.283	0.240	0.380	0.553	0.407
	coef.		0.216	0.800	0.019	0.663	0.764	0.872	0.949	0.689	0.408
Isotopic Ages	207Pb/206Pb	(i)	443.828	1058.640	1129.078	1070.953	1093.351	1089.897	1074.926	1090.347	1095.844
	±	(h)	7.135	8.638	87.627	8.428	4.584	2.652	2.398	8.933	10.588
	207Pb/235U	(i)	440.439	1095.048	954.309	1087.182	1091.835	1090.727	1197.114	1098.013	946.466
	±	(h)	1.103	4.762	22.732	3.732	2.368	1.809	2.497	3.870	3.340
	206Pb/238U	(i)	439.791	1113.452	880.300	1095.301	1091.075	1091.142	1265.933	1101.885	883.543
	±	(h)	0.751	6.271	20.496	3.980	2.843	2.406	4.369	5.596	3.356
Raw Data	206Pb/204Pb Mean	(j)	203.053	164.203	30.129	320.746	471.811	817.040	123.694	101.498	120.077
	% Standard Error	(h)	0.040	0.109	0.028	0.192	0.147	0.138	0.130	0.071	0.045
	206Pb/207Pb Mean	(j)	7.855	6.213	1.830	8.390	9.445	10.745	5.268	4.644	5.161
	% Standard Error	(h)	0.014	0.035	0.012	0.122	0.045	0.026	0.010	0.014	0.036
	206Pb/205Pb Mean	(j)	19.272	11.450	3.884	8.643	31.363	43.090	33.200	24.700	2.450
	% Standard Error	(h)	0.033	0.063	0.019	0.184	0.129	0.111	0.119	0.070	0.019
	207Pb/205Pb Mean	(j)	2.454	1.844	2.123	1.031	3.321	4.010	6.301	5.320	0.475
	% Standard Error	(h)	0.030	0.068	0.022	0.218	0.127	0.112	0.052	0.073	0.038
	204Pb/205Pb Mean	(j)	0.088	0.063	0.115	0.025	0.060	0.046	0.224	0.216	0.018
	% Standard Error	(h)	0.092	0.144	0.075	0.204	0.162	0.155	0.289	0.194	0.058
	208Pb/205Pb Mean	(h)	9.041	5.557	21.171	3.158	7.735	8.110	21.401	17.988	1.506
	% Standard Error	(h)	0.035	0.066	0.019	0.172	0.128	0.114	0.047	0.071	0.021
	202Pb/205Pb Mean	(j)	1.100	1.100	1.100	1.100	1.100	1.100	1.100	1.100	1.100
	% Standard Error	(h)	0.100	0.100	0.100	0.100	0.100	0.100	0.100	0.100	0.100
	238U/235U Mean	(j)	2.885	0.649	0.130	0.526	1.912	2.666	1.532	1.280	0.175
	% Standard Error	(h)	0.012	0.185	0.013	0.020	0.020	0.019	0.051	0.104	0.125
	233U/235U Mean	(j)	1.013	1.024	1.035	1.032	1.022	1.013	1.024	1.025	1.032
	% Standard Error	(h)	0.016	0.136	0.003	0.009	0.022	0.021	0.059	0.120	0.035
	238U/233U Mean	(j)	2.848	0.634	0.126	0.510	1.872	2.630	1.496	1.250	0.170
	% Standard Error	(h)	0.014	0.208	0.013	0.019	0.021	0.017	0.046	0.137	0.136

(a) labels for fractions composed of a cluster of titanite grains or fragments.

(b) Weight of 535 double spike added to each fraction

(c) Nominal U and total Pb concentrations subject to uncertainty in photomicrographic estimation of weight and partial dissolution during chemical abrasion.

(d) Model Th/U ratio calculated from radiogenic 208Pb/206Pb ratio and 207Pb/235U age.

(e) Pb* and Pbc represent radiogenic and common Pb, respectively; mol % ^{206}Pb* with respect to radiogenic, blank and initial common Pb.

(f) Measured ratio corrected for spike and fractionation only.

(g) Corrected for fractionation, spike, and common Pb; up to 1 pg of common Pb was assumed to be procedural blank: 206Pb/204Pb = 18.60 ± 0.80%; 207Pb/204Pb = 15.69 ± 0.32%; 208Pb/204Pb = 38.51 ± 0.74% (all uncertainties 1-sigma). Excess over blank was assigned to initial common Pb.

(h) Errors are 2-sigma, propagated using the algorithms of Schmitz and Schoene (2007) and Crowley et al. (2007).

(i) Calculations are based on the decay constants of Jaffey et al. (1971). 206Pb/238U and 207Pb/206Pb ages corrected for initial disequilibrium in 230Th/238U using Th/U [magma] = 3.

(j) Data which has been selected through Tripoli and subjected to a 2-sigma filter, but which has not been corrected for fractionation, spike, or Pb.

Table A1 Continued Samples: KSH Tail, LLNO10-01, LLNO10-02, LLNO10-03, LLNO11-08, and LLNO11-10. Raw and processed data used for calculations.

			MallardCreek_A	MIC1500_B	MIC1500_C	MIC1500 _D	N32_A	N32_B	N32_D	Salem_A	Salem_B
Compositional	Spike weight	(b)	0.090	0.020	0.020	0.020	0.020	0.020	0.020	0.090	0.090
Parameters	U ppm	(c)	204407.540	3534.331	1518.973	4338.336	67601.770	73992.941	84655.571	64902.039	56202.946
	Th/U	(d)	1.418	0.301	0.320	0.280	1.434	1.290	1.413	1.638	1.699
	Pb ppm	(c)	24388.131	705.611	384.041	719.708	13931.948	14802.141	17435.994	8824.431	8583.096
	206Pb* x 10-13 mol	(e)	758.390	9.678	4.085	11.892	436.793	477.094	544.298	138.114	118.902
	mol% 206Pb*	(e)	0.986	0.627	0.540	0.691	0.991	0.991	0.988	0.724	0.678
	Pb*/Pbc	(e)	25.877	0.484	0.337	0.638	43.342	39.222	31.457	1.032	0.838
	Pbc (pg)	(e)	907.516	475.621	287.357	439.531	314.230	368.051	537.259	4344.116	4669.798
	206Pb/204Pb	(f)	1287.235	49.289	39.978	59.473	2128.876	1986.517	1556.606	66.667	57.053
Radiogenic	208Pb/206Pb	(g)	0.440	0.096	0.096	0.088	0.439	0.395	0.433	0.517	0.540
Isotope Ratios	207Pb/206Pb	(g)	0.058	0.056	0.052	0.055	0.070	0.070	0.070	0.053	0.053
	% err	(h)	0.051	2.529	3.530	1.708	0.144	0.026	0.117	1.449	1.732
	207Pb/235U	(g)	0.714	0.510	0.462	0.498	1.499	1.493	1.489	0.371	0.371
	% err	(h)	0.412	2.789	3.326	1.585	0.328	0.193	0.382	1.336	1.582
	206Pb/238U	(g)	0.089	0.066	0.064	0.066	0.155	0.155	0.154	0.051	0.051
	% err	(h)	0.409	1.699	1.358	0.727	0.297	0.189	0.366	0.623	0.758
	coef.		0.992	0.450	0.049	0.053	0.898	0.991	0.952	0.044	0.032
Isotopic Ages	207Pb/206Pb	(i)	536.228	464.441	285.642	411.863	933.191	929.214	929.722	318.318	331.965
	±	(h)	1.107	56.039	80.708	38.187	2.958	0.531	2.395	32.933	39.282
	207Pb/235U	(i)	546.847	418.318	385.948	410.623	929.885	927.442	925.864	320.529	320.565
	±	(h)	1.743	9.563	10.678	5.352	1.997	1.172	2.322	3.672	4.349
	206Pb/238U	(i)	549.398	410.001	402.880	410.403	928.491	926.696	924.246	320.833	318.998
	±	(h)	2.152	6.749	5.301	2.890	2.567	1.631	3.149	1.948	2.357
Raw Data	206Pb/204Pb Mean	(j)	1282.319	49.151	39.851	59.302	2121.977	1980.383	1552.236	66.499	56.912
	% Standard Error	(h)	0.045	0.081	0.058	0.045	0.272	0.058	0.084	0.027	0.027
	206Pb/207Pb Mean	(j)	14.408	2.843	2.391	3.331	13.018	12.960	12.631	3.675	3.233
	% Standard Error	(h)	0.011	0.051	0.045	0.039	0.030	0.006	0.011	0.011	0.011
	206Pb/205Pb Mean	(j)	30.428	2.748	1.347	3.064	78.413	85.701	98.026	7.544	6.940
	% Standard Error	(h)	0.020	0.070	0.032	0.032	0.145	0.092	0.173	0.020	0.019
	207Pb/205Pb Mean	(j)	2.112	0.966	0.564	0.920	6.025	6.613	7.763	2.053	2.146
	% Standard Error	(h)	0.022	0.075	0.053	0.052	0.152	0.034	0.073	0.022	0.022
	204Pb/205Pb Mean	(j)	0.021	0.051	0.031	0.047	0.031	0.039	0.056	0.102	0.111
	% Standard Error	(h)	0.061	0.081	0.075	0.052	0.242	0.117	0.138	0.039	0.094
	208Pb/205Pb Mean	(h)	14.083	2.294	1.356	2.153	35.445	35.081	44.230	7.138	7.176
	% Standard Error	(h)	0.020	0.060	0.029	0.034	0.159	0.035	0.073	0.020	0.020
	202Pb/205Pb Mean	(j)	1.100	1.100	1.100	1.100	1.100	1.100	1.100	1.100	1.100
	% Standard Error	(h)	0.100	0.100	0.100	0.100	0.100	0.100	0.100	0.100	0.100
	238U/235U Mean	(j)	3.881	0.316	0.141	0.387	5.698	6.212	7.079	1.266	1.096
	% Standard Error	(h)	0.102	0.601	0.046	0.041	0.010	0.007	0.021	0.033	0.022
	233U/235U Mean	(j)	1.007	1.035	1.034	1.034	0.993	0.989	0.981	1.024	1.027
	% Standard Error	(h)	0.106	0.212	0.007	0.028	0.013	0.008	0.029	0.031	0.021
	238U/233U Mean	(j)	3.856	0.304	0.137	0.374	5.740	6.283	7.220	1.237	1.067
	% Standard Error	(h)	0.113	0.577	0.046	0.038	0.010	0.008	0.021	0.026	0.023

(a) labels for fractions composed of a cluster of titanite grains or fragments.

(b) Weight of 535 double spike added to each fraction

(c) Nominal U and total Pb concentrations subject to uncertainty in photomicrographic estimation of weight and partial dissolution during chemical abrasion.

(d) Model Th/U ratio calculated from radiogenic 208Pb/206Pb ratio and 207Pb/235U age.

(e) Pb* and Pbc represent radiogenic and common Pb, respectively; mol % ^{206}Pb* with respect to radiogenic, blank and initial common Pb.

(f) Measured ratio corrected for spike and fractionation only.

(g) Corrected for fractionation, spike, and common Pb; up to 1 pg of common Pb was assumed to be procedural blank: 206Pb/204Pb = 18.60 ± 0.80%; 207Pb/204Pb = 15.69 ± 0.32%; 208Pb/204Pb = 38.51 ± 0.74% (all uncertainties 1-sigma). Excess over blank was assigned to initial common Pb.

(h) Errors are 2-sigma, propagated using the algorithms of Schmitz and Schoene (2007) and Crowley et al. (2007).

(i) Calculations are based on the decay constants of Jaffey et al. (1971). 206Pb/238U and 207Pb/206Pb ages corrected for initial disequilibrium in 230Th/238U using Th/U [magma] = 3.

(j) Data which has been selected through Tripoli and subjected to a 2-sigma filter, but which has not been corrected for fractionation, spike, or Pb.

Table A1 Continued Samples: Mallard Creek, MIC1500, N32, and Salem. Raw and processed data used for calculations.

		(a)	SHF10-02_D	Thai_C-146_A	Thai_C-146_B	Thai146B_C	ThaiC146B_D	Triangle_A	Triangle_B
Compositional	Spike weight	(b)	0.075	0.020	0.020	0.020	0.001	0.001	0.001
Parameters	U ppm	(c)	10404.387	47109.970	47820.747	42079.236	41175.493	77626.645	62751.828
	Th/U	(d)	0.535	2.488	2.602	2.716	2.537	0.525	0.812
	Pb ppm	(c)	1759.618	2555.810	2800.594	2565.220	2767.026	7411.507	6803.802
	206Pb* x 10-13 mol	(e)	18.982	46.520	47.319	41.565	41.637	269.191	219.728
	mol% 206Pb*	(e)	0.551	0.838	0.810	0.798	0.755	0.973	0.955
	Pb*/Pbc	(e)	0.377	2.434	2.049	1.958	1.486	10.907	6.998
	Pbc (pg)	(e)	1277.862	744.302	918.712	867.235	1113.052	622.545	850.816
	206Pb/204Pb	(f)	40.947	113.293	96.596	91.165	75.192	674.925	410.512
Radiogenic	208Pb/206Pb	(g)	0.176	0.831	0.871	0.922	0.867	0.165	0.255
Isotope Ratios	207Pb/206Pb	(g)	0.054	0.052	0.052	0.052	0.053	0.058	0.058
	% err	(h)	4.553	0.746	0.902	0.997	1.191	0.105	0.234
	207Pb/235U	(g)	0.327	0.168	0.169	0.171	0.177	0.664	0.671
	% err	(h)	4.535	0.696	0.862	0.945	1.097	0.176	0.272
	206Pb/238U	(g)	0.044	0.024	0.024	0.024	0.024	0.083	0.084
	% err	(h)	1.363	0.318	0.373	0.443	0.530	0.147	0.160
	coef.		0.137	0.065	0.108	0.114	0.058	0.802	0.518
Isotopic Ages	207Pb/206Pb	(i)	378.886	266.230	272.166	306.566	328.310	525.241	527.788
	±	(h)	102.384	17.120	20.668	22.713	27.025	2.313	5.119
	207Pb/235U	(i)	287.204	157.984	158.658	160.619	165.599	516.831	521.232
	±	(h)	11.345	1.018	1.267	1.404	1.677	0.714	1.110
	206Pb/238U	(i)	276.063	150.857	151.157	150.891	154.435	514.930	519.737
	±	(h)	3.683	0.475	0.557	0.661	0.809	0.729	0.801
Raw Data	206Pb/204Pb Mean	(j)	40.823	112.996	96.351	90.932	75.006	671.853	408.906
	% Standard Error	(h)	0.132	0.028	0.069	0.041	0.025	0.050	0.113
	206Pb/207Pb Mean	(j)	2.435	5.530	4.919	4.696	4.042	12.599	10.717
	% Standard Error	(h)	0.172	0.012	0.031	0.014	0.010	0.020	0.059
	206Pb/205Pb Mean	(j)	1.636	9.884	10.402	9.267	9.810	10.945	9.098
	% Standard Error	(h)	0.113	0.020	0.047	0.032	0.020	0.017	0.056
	207Pb/205Pb Mean	(j)	0.672	1.787	2.115	1.973	2.427	0.869	0.848
	% Standard Error	(h)	0.182	0.022	0.061	0.033	0.023	0.026	0.077
	204Pb/205Pb Mean	(j)	0.036	0.081	0.094	0.096	0.118	0.015	0.020
	% Standard Error	(h)	0.134	0.047	0.145	0.050	0.069	0.057	0.119
	208Pb/205Pb Mean	(h)	1.684	10.194	11.426	10.685	11.392	2.369	3.054
	% Standard Error	(h)	0.117	0.020	0.050	0.033	0.021	0.020	0.060
	202Pb/205Pb Mean	(j)	1.100	1.100	1.100	1.100	1.100	1.100	1.100
	% Standard Error	(h)	0.100	0.100	0.100	0.100	0.100	0.100	0.100
	238U/235U Mean	(j)	0.251	4.025	4.081	3.615	3.529	1.506	1.219
	% Standard Error	(h)	0.066	0.015	0.005	0.032	0.023	0.036	0.024
	233U/235U Mean	(j)	1.032	1.005	1.005	1.007	1.009	1.024	1.027
	% Standard Error	(h)	0.023	0.017	0.008	0.047	0.036	0.036	0.021
	238U/233U Mean	(j)	0.244	4.005	4.061	3.590	3.498	1.472	1.187
	% Standard Error	(h)	0.065	0.013	0.006	0.031	0.029	0.031	0.031

(a) labels for fractions composed of a cluster of titanite grains or fragments.

(b) Weight of 535 double spike added to each fraction

(c) Nominal U and total Pb concentrations subject to uncertainty in photomicrographic estimation of weight and partial dissolution during chemical abrasion.

(d) Model Th/U ratio calculated from radiogenic 208Pb/206Pb ratio and 207Pb/235U age.

(e) Pb* and Pbc represent radiogenic and common Pb, respectively; mol % ^{206}Pb* with respect to radiogenic, blank and initial common Pb.

(f) Measured ratio corrected for spike and fractionation only.

(g) Corrected for fractionation, spike, and common Pb; up to 1 pg of common Pb was assumed to be procedural blank: 206Pb/204Pb = 18.60 ± 0.80%; 207Pb/204Pb = 15.69 ± 0.32%; 208Pb/204Pb = 38.51 ± 0.74% (all uncertainties 1-sigma). Excess over blank was assigned to initial common Pb.

(h) Errors are 2-sigma, propagated using the algorithms of Schmitz and Schoene (2007) and Crowley et al. (2007).

(i) Calculations are based on the decay constants of Jaffey et al. (1971). 206Pb/238U and 207Pb/206Pb ages corrected for initial disequilibrium in 230Th/238U using Th/U [magma] = 3.

(j) Data which has been selected through Tripoli and subjected to a 2-sigma filter, but which has not been corrected for fractionation, spike, or Pb.

Table A1 Continued Samples: SHF10-02, ThaiC-146 and Triangle. Raw and processed data used for calculations.

Sample Name	Lithology	Rock Unit	Geologic Setting	Location	Latitude and Longitude
BAK911	eclogite	Lick Ridge eclogite	metamorphic - high P	North Carolina	N/A
C221	granite	Waxhaw granite	Carolina zone granite	South Carolina	34°53'51.39" N, 80°48'12.35" W (GHSZ01-10)
Cabarrus	tonalite		Charlotte Concord-Salisbury	North Carolina	35.404859,-80.704303
Cotton Grove		Cotton Grove granite		North Carolina	35.7325602, -80.239592
Jamestown	tonalite	Greensboro igneous complex	Carolina terrane	North Carolina	35.962672,-79.919247
JR82-67	trondjhemite	Ankepura trondjhemite	Archean TTG suite, Dhawar craton	India	N/A
KSH68	granodiorite	Ellisville pluton "tail"	subduction pluton	Virginia	N38.07267,W77.92470
KSH86	granodiorite	Ellisville pluton "body"	subduction pluton	Virginia	N37.96328,W78.02464
LLN011-10	Younger Granite	Llano granite	Mesoproterozoic collisional granite	central Texas	0525109, 3375732 (N side of FM 965 at South Crabapple Creek)
LLNO10-01	Kingsland quarry	Llano granite	Mesoproterozoic collisional granite	central Texas	N/A
LLNO10-02	Summerland Dr quarry	Llano granite	Mesoproterozoic collisional granite	central Texas	N/A
LLNO10-03	pegmatitic phase of Lone Grove	Llano granite	Mesoproterozoic collisional granite	central Texas	N/A
LLNO11-08	Younger Granite	Llano granite	Mesoproterozoic collisional granite	central Texas	0526779, 3397642 (East Side of HY 2323 between Llano Co. Roads 118 & 117)
Mallard Creek	tonalite		Charlotte terrane basement	North Carolina	35.325508,-80.720601
MIC1500		Lick Ridge amphibolite	metamorphic - amphibolite facies	North Carolina	N/A
N32	calc-silicate	Novillo calc-silicate	moderate regional metamorphic terrane	Mexico	98°14.48 , 23°29.38
Salem	syenite	Churchland granite	Charlotte_Alleghenian	North Carolina	36.030478,-80.105091
SHF10-02	Rhyolite	felsic metavolcanic lens	Spring Hope terrane	North Carolina	N36° 12.6837', W078° 12.3472'
Thai C-146B	calc-silicate	Mae Wang calc-silicate	high-grade metamorphic	Thailand	collected near km 19 along the road from San Pa Tong to Samoeng, southwest of Chiang Mai (Macdonald et al., 2010)
Triangle	Andesite	meta-igneous, greenschist facies	Charlotte terrane basement	North Carolina	35.432453,-81.022661

Table A2 Sample description, setting and location.